Spinup toward Communication between Large Oceanic Subpolar and Subtropical Gyres

RICHARD SCHOPP

IFREMER Centre de Brest, Brest, France

(Manuscript received 31 August 1987, in final form 21 March 1988)

ABSTRACT

An interpretation in terms of planetary waves is proposed, which sheds light on the dynamics underlying the large-scale cross-gyre geostrophic flow recently developed in a two-layer ventilated thermocline model.

The cross-gyre communication flow is the result of an arrested nondispersive baroclinic Rossby wave in the presence of zonal Sverdrup transport along the line of vanishing Ekman pumping. A baroclinic adjustment is described in which a resting ocean settles to a steady communicating solution.

1. Introduction

The aim of this paper is to give some insight into the role nonlinear Rossby waves play in the maintenance of large-scale steady subpolar-subtropical cross-gyre flows found by Pedlosky (1984) and Schopp and Arhan (1986, hereafter SA) and to propose a process able to spin up a stratified ocean at rest toward such solutions.

Pedlosky (1984) and SA have recently extracted large-scale cross-gyre flow solutions from the inviscid ventilated thermocline layer model (Luyten et al. 1983, hereafter LPS). These nonlinear internal modes allow an exchange of midocean waters at the zero wind stress curl line, defined as the zonal boundary between the subpolar gyre where Ekman upwelling takes place and the subtropical gyre where Ekman downwelling takes place. Their solutions are entirely specified by imposing cross-gyre flow, i.e., by applying the appropriate cross-gyre boundary conditions in their model: either the correct potential vorticity distribution on the gyre separation line or on the western boundary, or the specification of the appropriate outcropping line in the subpolar gyre. The flow patterns obtained are nonunique, since the LPS model leads to equally consistent solutions without communication between gyres. Therefore, one may wonder whether a solution with no communication would be more appropriate to the actual ocean. To remove this ambiguity, one may reduce the question to whether a stratified ocean with no communication would be able, under some time adjustment process, to settle toward the steady state of cross-gyre flow.

This question may be answered by recalling the role played by Rossby waves in LPS-type steady models. Luyten and Stommel (1985, 1986a,b) observed a subtle interaction between the nondispersive internal Rossby wave and the mean zonal Sverdrup transport leading to the appearance of singular points in large-scale layered models. At these points, the nondispersive Rossby wave speed is exactly opposed to the eastward mean zonal current. Due to nonlinear propagation of Rossby waves, this balance can be applied on a nonzero extension region along the gyre separation line and will lead to the internal mode dynamics discussed in section 2: a nonlinear, nondispersive baroclinic Rossby wave arrested by an opposite-directed zonal mean current.

Further, the crucial role played by the nonlinearity of the Rossby wave for the existence of these steady communicating solutions enables us to isolate a simple mechanism—nonlinear baroclinic adjustment—which allows the ocean to evolve from a resting state toward the cross-gyre flow regime. The time scale on which the ocean reacts to perturbations will be given by the propagation of the long baroclinic Rossby wave. Fixing only a time scale is not sufficient to isolate a tractable problem, the latter being dependent on the spatial scale relative to the internal Rossby deformation radius. Luyten and Stommel (1986c) studied such transient regimes by considering planetary spatial scales (of about the width of an ocean basin) and therefore kept only the nonlinear steepening term of baroclinic Rossby wave propagation. The importance of this term comes from the fact that isopycnal surfaces can present significant vertical excursions. Thus, the wave feels layer thickness variations and changes speed while propagating. Since they need internal Rossby wave lengths comparable to the width of an ocean basin, the solutions proposed by these authors cannot account for smaller structures, which seem to be more responsible for oceanic variability. In this study, we consider smaller spatial scales of about 200 km, but nevertheless greater than the internal deformation radius, in order to keep the nonlinear character of wave propagation.

Corresponding author address: Dr. Richard Schopp, School of Oceanography WB-10, University of Washington, Seattle, WA 98195.

This scale is that of "intermediate regimes" or "IG equations" (Charney and Flierl 1981; Williams and Yamagata 1984), in which the dispersive term due to local variation of relative vorticity is of the same order as the nonlinear propagation term. This dispersive term prevents the waves from breaking, a possibility not allowed at very large scales. Likewise, coherent isolated structures can appear in the form of solitary waves in this dispersion/nonlinearity balance (Charney and Flierl 1981).

In section 3a, equations for the baroclinic and barotropic modes are derived in a two-layer model. The interface (or baroclinic mode) presents an equation of regularized long-wave type (Benjamin et al. 1972) in a variable mean zonal current, whereas the surface evolves under the effect of dispersive Rossby waves, remaining nevertheless coupled to the interface equation. In sections 3b and 3c, this dynamics is applied to the zero wind curl line. Either communicating internal modes or solitary waves are obtained according to the signs and forms of perturbations initially imposed.

2. Cross-gyre communication condition

a. Equations

The physical model used is an inviscid two-layer LPS model above a resting lower ocean, as shown in Fig. 1. Layers 1 and 2 are in motion and layer 3 is at rest; y_W (or f_W, f being the coriolis parameter) is the line of vanishing wind stress curl taken zonal throughout this study and thus defining the separation line of the subpolar and subtropical gyres, and $y_1(x)$ [or $f_1(x)$] is the outcropping line of layer 2 in the subpolar gyre. The forcing, i.e., the wind stress curl $w_E(x, y)$ acts only on layers in contact with the sea surface. Since the flow is geostrophic, hydrostatic and incompressible, the velocities in the ventilated region (see Pedlosky 1987) are given by

$$u_2 = -\frac{\gamma_2}{f}\frac{\partial h}{\partial y} \tag{2.1a}$$

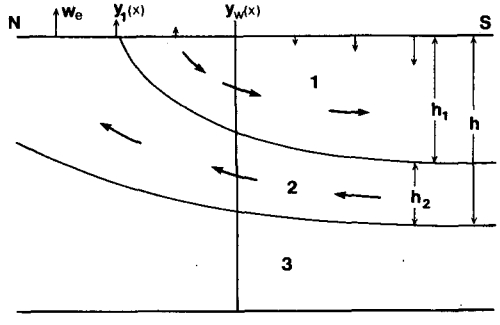

FIG. 1. A schematic meridional cross section of the model. The outcropping latitude $y_1(x)$ is located north of the zero wind-stress curl line y_W. Layer 3 is motionless.

$$v_2 = \frac{\gamma_2}{f}\frac{\partial h}{\partial x} \tag{2.1b}$$

$$u_1 = -\frac{\gamma_2}{f}\left[\frac{\partial h}{\partial y} + \frac{\gamma_1}{\gamma_2}\frac{\partial h_1}{\partial y}\right] \tag{2.1c}$$

$$v_1 = \frac{\gamma_2}{f}\left[\frac{\partial h}{\partial x} + \frac{\gamma_1}{\gamma_2}\frac{\partial h_1}{\partial x}\right], \tag{2.1d}$$

where $h = h_1 + h_2$ and $\gamma_n = g(\rho_{n+1} - \rho_n)/\rho_0$ ($n = 1, 2$). Vertical integration of the vorticity equation $\beta v_n = f(\partial w_n/\partial z)$, and use of (2.1b,d), lead to the Sverdrup transport equation

$$\frac{\partial}{\partial x}\left[h^2 + \frac{\gamma_1}{\gamma_2}h_1^2\right] = \frac{2f^2}{\beta\gamma_2}w_E = \frac{\partial}{\partial x}(D_0^2), \tag{2.2}$$

where

$$D_0^2(x, y) = -\frac{2f^2}{\beta\gamma_2}\int_x^{x_E} w_E(x', y)dx'. \tag{2.3}$$

Integration of (2.2) from the eastern wall taken as a meridian $x = x_E$, where u_1 and u_2 vanish, then yields

$$h^2 + \frac{\gamma_1}{\gamma_2}h_1^2 = D_0^2(x, y) + H_0^2, \tag{2.4}$$

where the constant H_0^2 is equal to $h^2(x_E)$ or $[h^2(x_E) + (\gamma_1/\gamma_2)h_1^2(x_E)]$, depending on whether $y_1(x)$ reaches the eastern boundary $[h_1(x_E) = 0]$ or not, $[h_1(x_E) \neq 0]$ and $h(x_E)$ and $h_1(x_E)$ are constant in the y-direction.

Conservation of potential vorticity in layer 2, $\mathbf{u}_2 \cdot \nabla(f/h_2) = 0$, added to the fact that the deeper layer 3 is at rest, implies that lines of constant potential vorticity are lines of constant h, i.e.,

$$f/h_2 = G(h). \tag{2.5}$$

The function $G(h)$ can be determined at the outcropping line y_1 where $h_2 = h$ and $f = f_1$, and is formally given by

$$\frac{f}{h_2} = \frac{f_1(h)}{h}. \tag{2.6}$$

The depth of layer 1 is then related to h by

$$h_1 = \left(1 - \frac{f}{f_1(h)}\right)h. \tag{2.7}$$

Using (2.7), (2.4) becomes

$$h^2 + \frac{\gamma_1}{\gamma_2}\left(1 - \frac{f}{f_1(h)}\right)^2 h^2 = D_0^2 + H_0^2. \tag{2.8}$$

Once $f_1(h)$ is given, the solution in the ventilated region can be computed by relations (2.7) and (2.8). Therefore, to solve the problem, one needs to know the potential vorticity along the outcropping line. This is achieved if the outcropping line $f_1(h)$ is prescribed,

the depth of layer 2 along this line being determined by the Sverdrup constraint and the eastern boundary condition in the one-layer moving region. In the communicating solution of SA, this line y_1 was not prescribed, and $f_1(h)$ was determined from another condition, namely cross-gyre communication.

The model presented will be used with the simplifying assumption that density jumps between layers are equal $\gamma_2 = \gamma_1$.

b. *Necessary condition for cross-gyre flow*

Schopp and Arhan (1986), after inserting (2.7) in (2.2), have shown that the Sverdrup constraint (2.2) can be rewritten as

$$hv_2\left[1+\left[1-\frac{f}{f_1(h)}\right]^2+h\frac{f}{f_1{}^2(h)}\left[1-\frac{f}{f_1(h)}\right]\frac{df_1}{dh}\right] = \frac{f}{\beta}w_E, \quad (2.9)$$

and that communication, i.e., $v_2 \neq 0$ at the line y_W where $w_E = 0$, requires the term in brackets to vanish along this line y_W. Thus, they defined the communication condition as

$$1+\left[1-\frac{f}{f_1(h)}\right]^2+h\frac{f}{f_1{}^2(h)}\left[1-\frac{f}{f_1(h)}\right]\frac{df_1}{dh}=0 \quad \text{at } f=f_W. \quad (2.10)$$

Integrated, this first-order differential equation leads to the unknown function $f_1(h)$:

$$1-\frac{f_W}{f_1(h)}=\left[\frac{H_0{}^2}{h^2}-1\right]^{1/2}, \quad (2.11)$$

which is valid for $f_W \leqslant f_1$ and $(H_0/\sqrt{2}) \leqslant h \leqslant H_0$. They arrived at the conclusion that imposing communication uniquely determines the function $f_1(h)$ and consequently, they were able to compute a deep northward cross-gyre flow outcropping in the eastern subpolar gyre. In their solution, SA assumed that (2.10) can be integrated up to the eastern boundary, i.e., that the internal mode extends up to x_E. Should this not be true, i.e., should v_2 vanish over some finite region as we approach the eastern edge of the gyre, then the outcropping line could not reach the eastern boundary [i.e., $h_1(x_E) \neq 0$] and would be forced to bend northward, following a constant $D_0{}^2$ line. East of this line layer 2 would be at rest. This would then lead to the existence of a strong, warm upper-layer northward flow around the basin confined east of the communicating gap. Figure 2 illustrates this case.

As will be seen in the next section, the mathematical condition defining communication represents a nondispersive internal Rossby wave arrested by a mean zonal current.

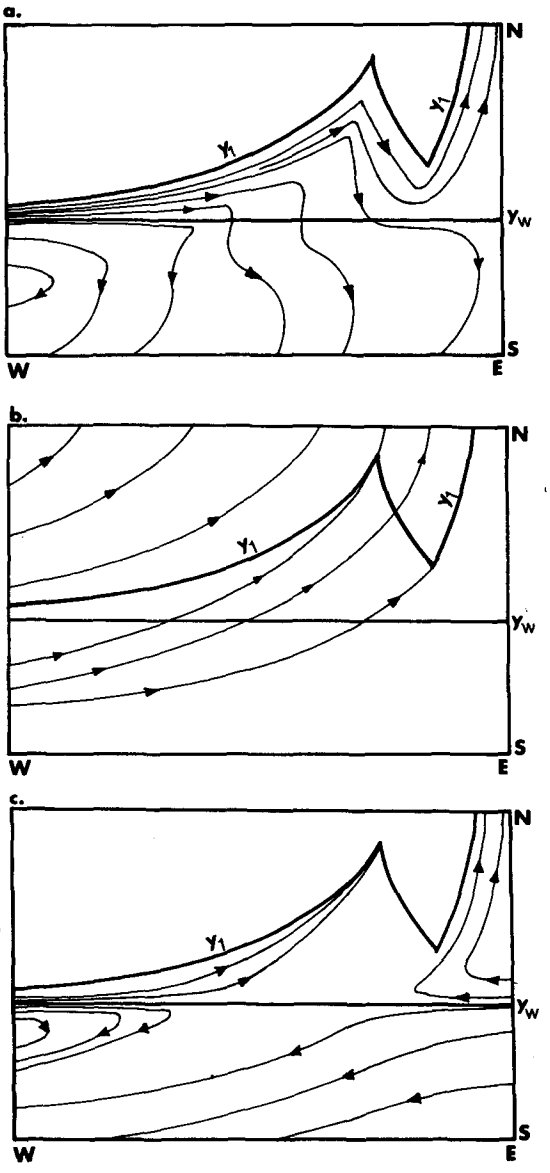

FIG. 2. Schematic circulation patterns for the case in which cross-gyre flow does not extend up to the eastern boundary: (a) upper-layer flow, (b) deep-layer flow, (c) resulting characteristics.

c. *Physical interpretation of the internal mode*

The main characteristic of the above-mentioned solution is that the line $f_1(h)$ [or $G(h)$] has not been specified a priori, but rather is a result of the dynamics itself due to imposing cross-gyre communication between subtropical and subpolar gyres, i.e., by canceling the term in brackets in (2.9) along line y_W. In spite of plausible results obtained for the eastern North Atlantic circulation by SA, this mathematical formulation of communication requires a more detailed examination of the physical content. This is the aim of this section.

1) CONDITION REQUIRED FOR COMMUNICATION

To make the physical meaning clearer, we compute the mean zonal velocity $u = [h_1u_1 + h_2u_2]/h$. Using equations (2.1a, c) and (2.7), the following value is obtained for u:

$$u = -\frac{\beta\gamma_2}{f}\left[1 + \left(1 - \frac{f}{f_1}\right)^2 + h\frac{f}{f_1^2}\left(1 - \frac{f}{f_1}\right)\frac{df_1}{dh}\right] \times \frac{\partial h}{\partial f} + \frac{\beta\gamma_2}{f}\left(1 - \frac{f}{f_1}\right)\frac{h}{f_1}. \quad (2.12)$$

Applying condition (2.10) to (2.12), i.e., canceling the term in brackets, implies the following equality:

$$u = \frac{\beta\gamma_2}{f}\left(1 - \frac{f}{f_1}\right)\frac{h}{f_1} \quad \text{at} \quad f = f_W,$$

which by means of (2.6) and (2.7) leads to

$$u = \frac{\beta\gamma_2}{f^2}\frac{h_1h_2}{h}. \quad (2.13)$$

The right-hand side of (2.13) is the nonlinear phase speed c of the nondispersive internal Rossby wave only, so the communication condition can be simply expressed as a baroclinic long Rossby wave arrested by an eastward mean zonal current:

$$u = -c. \quad (2.14)$$

This turns out to be the critical condition of Rossby repellor in the characteristic equation of Luyten and Stommel (1985, 1986a). In a two-layer model over a resting ocean, they have shown on the one hand, a region in which information comes from the eastern boundary (the internal Rossby wave phase speed being greater than the mean zonal current), and on the other, a region in which the characteristics come from the western boundary layer (the mean current this time being greater). At y_W, both regions are separated by a point they have named Rossby repellor. Since condition (2.14) applies to one point only of line y_W in their model, they have included interfacial thermal fluxes to achieve water transfer from one gyre to the other (Luyten and Stommel, 1986b). In contrast, in the aforementioned solution as well as in that of Pedlosky (1984), condition (2.14) continuously applies along line y_W with wind forcing only. Recall that Rhines (1986) has also shown in a two-layer unforced model that condition (2.14) is required to generate meridional currents.

The reason the internal mode can exist and possess a zonal extension is linked to variations of h_1 and h_2, which allow the Rossby wave phase speed c to vary in relation to longitude, so as to exactly balance the westward increasing mean zonal current proportional to $\partial D_0^2/\partial y$. However, this balance cannot go on westward indefinitely. The fact that the Rossby wave speed exhibits a maximum and that the internal mode must satisfy the Sverdrup relation $h^2 + h_1^2 = H_0^2$ together impose a constraint on the choice of h_1 and h_2, and therefore limit possible values of phase speed c. Replacing h_1 and h_2 by their values in terms of h by means of the Sverdrup relation, the latter can be written

$$-\frac{hc}{H_0^2} = \frac{\beta\gamma_2}{f^2}\left[\frac{(H_0^2 - h^2)^{1/2}}{H_0}\frac{h}{H_0} - \frac{(H_0^2 - h^2)}{H_0^2}\right].$$

This relation is illustrated in Fig. 3. The expression hc shows a maximum for a value h^2/H_0^2 of $(2 + \sqrt{2})/4$, corresponding indeed to that obtained by SA, which in their model determined the western boundary of the ventilated region along y_W. The branches of this curve to either side of the maximum illustrate the two possible solutions of the internal mode (northward flow and southward flow in the deeper layer). The arrow in Fig. 3 indicates the variation of wave speed in the westward direction for a typical applied wind forcing, for which the Sverdrup mean zonal flow increases westward. For both solutions, the western limit is located at the longitude where hc reaches its extremum and beyond which it can no longer equal the zonal transport, which increases westward. It can be noticed in this region that $u > -c$, and therefore, that information carried by the Rossby wave propagates eastward. The solution can also present an eastern boundary, such as the one developed by Pedlosky (1984). Since the boundary conditions $h_1(x_E)$ and $h_2(x_E)$ are chosen as nonvanishing on the eastern boundary, the wave speed c at x_E will be different from zero while u vanishes so that the ventilated region can only exist from the longitude where u reaches the critical value $c(x_E)$. This more general case determines a second region at y_W, where information comes from the eastern boundary: $u < -c$, contrary to the northward solution developed in SA, where c vanishes at x_E (h_1 being forced to stay zero at x_E) and is able to balance the mean zonal current up from the eastern boundary [$u(x_E) = 0$]. In Fig. 3, boundary values of h equal to H_0 and $(2^{1/2}/2)H_0$, h

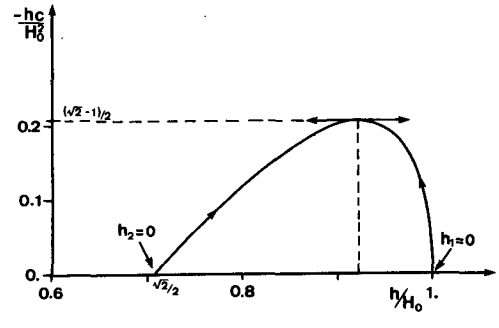

FIG. 3. Curve representing the Rossby phase speed $-hc/H_0^2$ [unities $-(\gamma_2\beta/f^2)^{-1}$] as a function of the depth h/H_0. The maximum observed divides the curve into two branches, where each represents the possible values for the two cross-gyre solutions in SA. The right branch is the current to the north in the deeper layer; the arrow gives the westward direction.

enabling communication, can also be noticed. Likewise, singularities observed in the model come from the nonlinear Rossby wave speed c, presenting a shock wave on the western boundary (intersection of characteristics).

We have shown that all internal mode properties along the latitude of the zero wind curl line can be interpreted as an arrested wave from the sole relation (2.14). Let us now try to extend this formulation to the whole ocean basin.

2) CHARACTERISTIC EQUATION

We again develop the characteristic equation of Luyten and Stommel (1986a) and apply it to both gyres.

Conservation of potential vorticity in layer 2 can be rewritten by means of (2.1a, b) as

$$J(h_2, h) + \frac{\beta}{f} h_2 h_x = 0,$$

or, knowing that $h = h_1 + h_2$, as

$$h_x h_{1y} - h_y h_{1x} + \beta/f h_2 h_x = 0, \qquad (2.15)$$

where the subscript x or y represents partial derivation. Multiplying (2.15) by $2h_1$ and using equation (2.4) yields

$$\left[-\frac{2\beta}{f} h_1 h_2 - \frac{\partial {D_0}^2}{\partial y} \right] h_x + \frac{2f^2 w_E}{\beta \gamma_2} h_y = 0. \qquad (2.16a)$$

In a more condensed form, the characteristic equation (2.16a) becomes

$$[hc + U] h_x + V h_y = 0, \qquad (2.16b)$$

where $U = -\gamma_2/(2f) D_{0y}^2$ and $V = f/\beta w_E$ represent zonal and meridional Sverdrup transports, and

$$c = -\frac{\beta \gamma_2}{f^2} \frac{h_1 h_2}{h}$$

is the nondispersive internal Rossby wave speed.

On y_W, where the meridional Sverdrup transport V vanishes, equation (2.16b) reduces to

$$[hc + U] \frac{\partial h}{\partial x} = 0, \qquad (2.17)$$

whose two possible solutions are given by

- $\partial h/\partial x = 0$ or h = constant zonally, i.e., a zero meridional transport in layer 2 and therefore in layer 1, thus no communication in this case.
- $hc + U = 0$ or $c = -U/h = u$, i.e., communicating solution obtained in the preceding paragraph.

In addition to a solution in which the gyres are autonomous, this equation contains the internal mode as a particular solution. Since it is more general, (2.16) allows us to determine the characteristics of the whole basin. In fact, fixing values of the thicknesses $h = H_0$ and $h_1 \sim 0$ on the eastern boundary and $h = H_W$ on the western boundary, i.e., values giving the northward flow solution in SA, makes it possible to solve (2.16) easily, providing the characteristic trajectories (see Luyten and Stommel 1986b). Let us recall that only one condition can be imposed on the western boundary, since the Sverdrup transport is determined on the whole basin by the knowledge of eastern boundary conditions, and thus h_1 must satisfy the equation ${h_1}^2 + {H_W}^2 = {D_0}^2 + {H_0}^2$.

Figure 4 shows the characteristics emanating from both boundaries for the circulation developed in SA. These characteristics also represent lines of equal potential vorticity and, consequently, the field on which Rossby waves propagate in this two-layer model; three distinct regions can be observed:

- a region dominated by the eastern boundary, where $c > -u$;
- a second region dominated by the western boundary, where $c < -u$ in the vicinity of latitude y_W and $c > -u$ more southerly, (recall that layer 2 is at rest in these two regions);
- and a third region located between these two in which no information can come from either the eastern boundary or the western one and which corresponds to the ventilated domain of the northward communicating solution of SA.

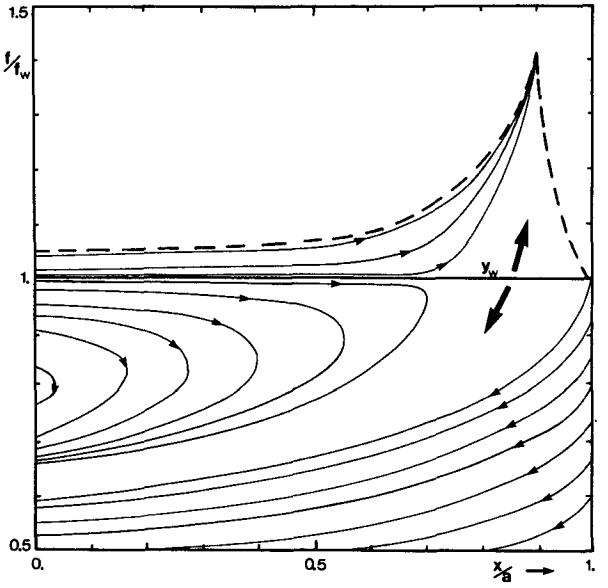

FIG. 4. Characteristics field of the deep northward cross-gyre solution in SA (realized with a model borrowed from H. Stommel). One can observe the two regions influenced by eastern and western boundaries. The ventilated region accepts no information from either the eastern or the western coast, but from the line y_W; arrows indicate information flow direction. (Basin width a = 6000 km; f_W = 1.11 10^{-4} s^{-1}; γ_2 = 0.01 m s^{-2}; $w_E = -w_0 \sin(\pi f/f_W)$; $w_0 = 10^{-4}$ cm s^{-1}; $H_0 = h(x_E)$ = 1200 m; $h_1(x_E) \sim 0$; $H_W \sim$ 1150 m.)

Since knowledge of the conditions on both eastern and western boundaries alone is insufficient to determine characteristics of the ventilated region, additional information is required. The origin of this information is the separation line y_W of both gyres. In fact, according to (2.16), information propagates northward from y_W in the subpolar gyre (V being positive) and southward from this line in the subtropical gyre (V being negative). However, the characteristic velocities are equal to zero along y_W, and no information can escape from this line. It can nevertheless be anticipated that simple perturbations generated along this line will propagate toward both gyres, and the observed steady circulation can be adjusted. The information-generating role of y_W was already implicit in the internal mode formulation, where the communication condition applied to y_W imposed circulation in the whole basin and fixed above all the subduction line localization.

Figure 2 schematically shows the characteristics for the case in which the cross-gyre flow does not extend up to the eastern edge of the basin. An eastward regime along the gyre separation line and in the subpolar gyre is seen.

An objection has often been raised to the specification of a subduction line in the subpolar gyre, where the vorticity distribution is determined at the course end, i.e., where the fluid column reaches the surface. Such a specification, it is claimed, requires a priori knowledge of the whole past history of this column. This objection is no longer justified when it is the information coming from y_W, which is largely responsible for the observed circulation. Likewise, the vorticity distribution applied along the eastern boundary in the second example of SA can be the result of the information carried by Rossby waves toward this region, thus enabling junction of current lines to the eastern boundary.

The qualitative contribution of the Rossby wave concept in this study, interpreting circulation in the Atlantic as a wave arrested by a current, enables us to account for the importance of the separation line of both gyres, which happens to be the place where information can be generated and propagated toward the inside of each gyre. The next section will propose a time-dependent model, using this wave notion to adjust the ocean to the steady circulation obtained previously.

3. Spinup toward communication

In this section, a time-dependent mechanism is proposed for which the ocean evolves from a stationary regime (where both subpolar and subtropical gyres are independent) to the preceding communicating steady state, under the effect of perturbations generated on the eastern and western basin boundaries.

a. Equations

Time introduction by means of internal long Rossby waves propagation in a two-layer model above a LPS-type resting ocean would require that we solve simultaneously two nonlinear coupled equations representing both baroclinic modes, the barotropic mode being given by the Sverdrup transport. To disregard this coupling, a single two-layer model with a flat bottom will be considered, which contains only one of these baroclinic modes.

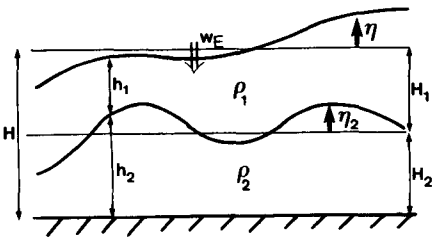

FIG. 5. Vertical section of the two-layer model.

The vertical structure of this ocean is schematically represented in Fig. 5.

The dynamics is assumed to be inviscid and in hydrostatic ($H/L \ll 1$) and geostrophic ($\epsilon = U/fL \ll 1$) balance. The velocities are then given by

$$fv_1 \approx gh_x \tag{3.1a}$$

$$fu_1 \approx -gh_y \tag{3.1b}$$

$$fv_2 \approx gh_x + g(\Delta\rho/\rho)h_{2x} \tag{3.1c}$$

$$fu_2 \approx -gh_y - g(\Delta\rho/\rho)h_{2y}, \tag{3.1d}$$

where $\Delta\rho/\rho = (\rho_2 - \rho_1)/\rho_0$, $h = h_1 + h_2$ and where the subscripts x, y and t represent partial derivations. The meaning of various quantities is illustrated in Fig. 5.

Vorticity equations for both layers are given by

Layer 1:

$$h_1\frac{\partial\xi_1}{\partial t} + h_1\mathbf{u}_1\cdot\nabla\xi_1 + h_1\beta v_1 - f\frac{\partial h_1}{\partial t} - f\mathbf{u}_1\cdot\nabla h_1 = fw_E, \tag{3.2a}$$

Layer 2:

$$h_2\frac{\partial\xi_2}{\partial t} + h_2\mathbf{u}_2\cdot\nabla\xi_2 + h_2\beta v_2 - f\frac{\partial h_2}{\partial t} - f\mathbf{u}_2\cdot\nabla h_2 = 0, \tag{3.2b}$$

where w_E represents the Ekman pumping, and $\xi_1 = \mathbf{k}\cdot\nabla\times\mathbf{u}_1$ and $\xi_2 = \mathbf{k}\cdot\nabla\times\mathbf{u}_2$ are the vertical components of the relative vorticity of each layer. Assuming spatial scales smaller than the earth's radius, $\beta L/f \ll 1$, these components become:

$$\xi_1 = (g/f)\nabla^2 h \quad \text{and}$$

$$\xi_2 = (g/f)\nabla^2[h + (\Delta\rho/\rho)h_2]. \tag{3.4}$$

Equations (3.2) will be nondimensionalized, and asterisks will be used to represent dimensional quantities.

Since the dynamics is geostrophic, thicknesses can be parameterized by (see Pedlosky 1987):

$$h^* = H \quad h = H[1 + \epsilon F\eta]$$
$$h_2^* = H \quad h_2 = H[H_2/H + \epsilon F_D(H_1H_2/H^2)\eta_2] \quad (3.6)$$
$$h_1^* = h^* - h_2^*,$$

where η and η_2 are surface and interface displacements, $F = (fL)^2/(gH) = L^2/L_E^2$ is the external Froude number, $L_E = (gH)^{1/2}/f$, the external deformation radius, $F_D = (fL)^2/(g'H_1H_2/H) = L^2/L_D^2$ the internal Froude number, $g' = g\Delta\rho/\rho$, the reduced gravity, and $L_D = (g'H_1H_2/H)^{1/2}/f$, the internal deformation radius.

The scaling has been performed so that η and η_2 are of the same order O(1).

The time scale has been chosen to give order 1 propagation of long linear baroclinic Rossby wave:

$$\frac{\omega}{f} = \frac{\beta_0}{F_D}, \quad (3.7)$$

i.e., linear phase speed $\beta L_D^2/(\omega L) \sim O(1)$, where $\beta_0 = \beta L/f$ represents the planetary parameter and ω the inverse of a time-scale T^{-1} (frequency).

The nonlinear propagation term, or steepening term, is of order ϵF_D and is small at the spatial scales used ($\approx$200 km, $\beta_0 \ll 1$). This term will nevertheless be kept (spatial scale greater than the internal Rossby radius, i.e., $F_D \gg 1$), since it allows the communicating solution to exist by being opposed to the mean zonal current variation. Notice that this term is neglected in quasi-geostrophy, where isopycnal surfaces cannot have significant vertical excursions and, therefore, do not allow Rossby waves to feel the layer thickness variations. At these scales, the dispersive term, of order F_D^{-1}, is of the same order and balances the nonlinear term in case the wave should present steepening. This balance is characteristic of solitary wave propagation. The spatial scale will thus be determined by the balance of both terms, the term in the ϵF_D being nevertheless able to dominate:

$$F_D^{-1} \leqslant \epsilon F_D. \quad (3.8)$$

Charney and Flierl (1981) have already shown the existence of solutions that propagate in the ocean in the form of solitary waves at these scales, when the nonlinear advection term is of the same order as the zonal dispersion term. Notice that this balance would require very low currents for large scales compared to the internal deformation radius, since dispersion decreases at large scales ($u \sim fL_D^4/L^3$); it is for this reason that nonlinearity is allowed to dominate in (3.8).

To filter out the nondispersive barotropic mode, we suppose further $\Delta\rho/\rho \ll F_D^{-1}$. This is essentially an instantaneous adjustment, at order 1, of the steady Sverdrup regime.

By adding (3.2a) and (3.2b) and considering only terms of order ϵF_D we obtain

$$\eta_x + H_2/H\eta_{2x} + \epsilon F_D H_1H_2/H^2\eta_2\eta_{2x} + F_D^{-1}\nabla^2[\eta_t + H_2/H\eta_{2t}] - \epsilon/\beta_0\{H_1/HJ(\nabla^2\eta, \eta) + H_2/HJ[\nabla^2(\eta + \eta_2), \eta + \eta_2]\} = w_E/(\epsilon\beta_0 fH). \quad (3.9)$$

Substituting this barotropic mode into the vorticity equation (3.2a) of layer 1, an equation for interface displacement η_2 or baroclinic mode is obtained:

$$\eta_{2t} - \eta_{2x} - \epsilon F_D(H_1 - H_2)/H\eta_2\eta_{2x} - F_D^{-1}\nabla^2\eta_{2t} - \epsilon F_D w_E/(\epsilon\beta_0 fH)\eta_2 - \epsilon/\beta_0 J(\nabla^2\eta, \eta) + \epsilon/\beta_0 J[\nabla^2(\eta + \eta_2), \eta + \eta_2] - \epsilon F_D/\beta_0 J(\eta_2, \eta) = w_E/(\epsilon\beta_0 fH_1). \quad (3.10)$$

A term in $(\epsilon F_D)^2 H_1H_2/H^2\eta_2{}^2\eta_{2x}$ has been neglected in this equation, (ϵF_D) being assumed to be small. This quadratic term is a higher order term in the baroclinic Rossby wave phase speed and will be taken into account subsequently in order to bring to the fore both internal modes observed in the steady communicating state. We might also note that the nonlinear part of the phase speed can be canceled in case $H_1 = H_2$, the Rossby wave phase speed possessing an extremum. But in view of the thermocline position in this two-layer model, as well as in the actual ocean, $H_1 \ll H_2$, this possibility will not be reached. It is sufficient that $(H_1 - H_2)/H \gg \epsilon F_D$ to justify neglecting the $\eta_2{}^2$ term noted above. Nevertheless, in LPS model where there is a deep layer at rest, both surface layers can present similar thicknesses and satisfy the extremum condition of Rossby wave propagation velocity (this extremum being exactly that obtained in the internal mode of Fig. 3).

Since this equation is too complex, an additional approximation will be made concerning the elimination of relative vorticity advection. This is achieved if

$$\epsilon/\beta_0 \ll \epsilon F_D. \quad (3.11)$$

Notice that this is the most constraining approximation for all derived equations.

Integrating the barotropic mode (3.9) with respect to longitude x, the free surface η can be expressed in terms of η_2:

$$\eta = -\frac{H_2}{H}\eta_2 - \epsilon F_D \frac{H_1H_2}{2H}\eta_2{}^2 - \frac{1}{F_D}\int_x \nabla^2\left(\eta_t + \frac{H_2}{H}\eta_{2t}\right)dx' + D_0{}^2 + K(y, t), \quad (3.12)$$

where

$$D_0{}^2 = -\int_x^{x_E} w_E/(\epsilon\beta_0 fH)dx'$$

and $K(y, t)$ is an integration constant that depends on the eastern boundary condition and thus will be supposed constant (i.e., no flow through the boundary).

The term represented by the integral in (3.12) is at maximum of order F_D^{-1} inside the fluid that is of interest, but it can nevertheless become significant on the western boundary where it is responsible for the formation of boundary layers. Also notice the appearance of the ventilated thermocline Sverdrup function $D_0{}^2$.

Substituting this value of η in (3.10) and neglecting any term in ϵ/β_0, we obtain

$$\eta_{2t} - \eta_{2x} - \epsilon F_D(H_1 - H_2)/H\eta_2\eta_{2x} - F_D^{-1}\nabla^2\eta_{2t} - \epsilon F_D w_E/(\epsilon\beta_0 fH)\eta_2 - \epsilon F_D/\beta_0 J(\eta_2, D_0{}^2) = w_E/(\epsilon\beta_0 fH_1), \quad (3.13)$$

where

- $\eta_{2t} - \eta_{2x}$ represents the nondispersive linear Rossby wave propagation;
- $-\epsilon F_D(H_1 - H_2)/H\eta_2\eta_{2x}$, the nonlinear contribution responsible for steepening and shock wave formation;
- $-F_D^{-1}\nabla^2\eta_{2t}$, the dispersion that enables steepening stabilization and solitary wave propagation;
- $-(\epsilon F_D)/\beta_0 J(\eta_2, D_0{}^2)$, the barotropic effect resulting when wind introduces a mean zonal current;
- the right-hand side is the wind forcing, which acts directly on the fluid column.
- the remaining term in η_2 is the correction of the direct forcing for nonsmall η_2 values.

Equation (3.13) contains only η_2 and can therefore be solved easily given initial conditions and boundary conditions. Once η_2 is determined, η is obtained by

$$\eta_x + F_D^{-1}\nabla^2\eta_t = -F_D^{-1}H_2/H\nabla^2\eta_{2t} - H_2/H\eta_{2x} - \epsilon F_D H_1 H_2/H^2\eta_2\eta_{2x} + w_E/(\epsilon\beta_0 fH), \quad (3.14)$$

or

$$\eta_{Bx} + F_D^{-1}\nabla^2\eta_{Bt} = w_E/(\epsilon\beta_0 fH),$$

where $\eta_B = \eta + (H_2/H)\eta_2 + \epsilon F_D H_1 H_2/(2H^2)\eta_2{}^2$ represents the nonlinear barotropic mode, which evolves under the influence of dispersive Rossby waves and which is forced by the wind. Notice that the barotropic mode is decoupled from the baroclinic mode.

Since communication is of interest, we shall apply (3.13) and (3.14) to the zero wind curl line.

b. *Regularized long-wave equation (RLWE) along y_W*

In order that line y_W be a place where information can be generated and spread toward both gyres, it is essential to reach the communicating steady solution along this line from an ocean at rest or from a flow pattern in which both gyres are separated. We apply (3.13) and (3.14) at y_W where Ekman pumping vanishes. We shall also suppose that the scale in y is larger than that in x, which will allow neglect of the y component dispersive term and simplify resolution, although this approximation is not very realistic. This gives

$$\eta_{2t} - \eta_{2x} - \epsilon F_D(H_1 - H_2)/H\eta_2\eta_{2x} - F_D^{-1}\eta_{2xxt} - \epsilon F_D/\beta_0 D_{0y}^2\eta_{2x} = 0, \quad (3.15)$$

where D_{0y}^2 represents Sverdrup zonal transport.

The w_E will be chosen as a linear function of latitude:

$$w_E = -w_0(1 - y_*/y_W),$$

which is indeed the approximation of a sinusoid when y tends toward y_W, and is therefore representative of the choice of w_E in SA. Thus, we have the following expression for the Sverdrup function:

$$D_0{}^2 = w_0/(\epsilon\beta_0 fH)(1 - y)(x_E - x),$$

with $x_E = 0$ and $y = y^*/y_W$. The zonal Sverdrup transport, which also represents the mean zonal velocity in this nondimensionalization, is given by

$$-D_{0y}^2 = -w_0/(\epsilon\beta_0 H)x, \quad x \leqslant 0. \quad (3.16)$$

Equation (3.15) for the baroclinic mode η_2 can therefore be rewritten as

$$\eta_{2t} - [1 + E_1\eta_2 + Ux]\eta_{2x} - E_2\eta_{2xxt} = 0, \quad (3.17)$$

where $E_1 = \epsilon F_D(H_1 - H_2)/H$; $E_2 = F_D^{-1}$; $U = F_D w_0/(\beta_0{}^2 fH)$.

With $U = 0$, (3.17) is the regularized long-wave equation (RLWE) or "BBM equation", analyzed in detail by Benjamin et al. (1972), and accepts solitary waves as solutions. Its structure is similar to the KDV equation (Korteweg and de Vries 1895), differing only in having a dispersive term of the form η_{2xxt} rather than η_{2xxx}. For more details on the solutions and properties of these equations, the reader is referred to Whitham (1974) and Dodd et al. (1982). Let us recall, however, that if a system governed by such dynamics is disturbed, the perturbation evolves toward a solitary wave train. Equation (3.17) presents an additional term, which is a function of longitude and is due to the mean zonal current $-Ux$. The effect of this term is to make the medium in which waves propagate inhomogeneous. It represents a damping term for the baroclinic mode, which can be seen with the following change of variable: $\psi = 1 + E_1\eta_2 + Ux$ leading to

$$\psi_t - \psi\psi_x - E_2\psi_{xxt} = -U\psi.$$

The free surface equation will be given by

$$\eta_x + E_2\eta_{xxt} = H_2/H \times [-E_2\eta_{2xxt} - \eta_{2x} - \epsilon F_D H_1/H\eta_2\eta_{2x}], \quad (3.18)$$

and its evolution will be governed by dispersive barotropic Rossby waves, with dispersion relation ω

$= -(E_2k)^{-1}$, or dimensionally $w_* = -\beta/k$, k being the wavenumber.

The most significant remark to be made concerning Eq. (3.17) is that it contains the communication internal mode as a stationary solution: $c = 1 + E_1\eta_2 = -Ux$ (dimensionally $c = -u$) or

$$\eta_2 = -(1 + Ux)/E_1, \tag{3.19}$$

and in consequence, the steady free surface of this state will be given by (3.18):

$$\eta = (H_2/H)(U/E_1)\{[1 - H_1/(H_1 - H_2)]x - H_1/(H_1 - H_2)U/2x^2\} + K, \tag{3.20}$$

where K represents an integration constant given by the eastern boundary conditions.

The objective to be reached is to adjust this state by perturbing the other steady state, which is also a solution of (3.17) and in which η_2 is constant, i.e., both gyres are independent.

c. Numerical resolution—application

The application will concern an ocean whose interface along the zero wind curl line has no zonal variation. Perturbations will be performed on the eastern and western boundaries of the domain considered by specifying different thicknesses. Nevertheless, communication can exist in the basin only for a particular choice of parameters imposed by the presence of a communicating window in the basin. This choice amounts to assuming the existence of a region where information comes from the western boundary ($u > -c$) and one where it comes from the eastern boundary.

1) CHOICE OF PARAMETERS

According to the analysis in paragraph 3a, spatial scales must satisfy the following conditions:

$$\beta_0 \ll 1; \quad F_D^{-1} \leqslant \epsilon F_D; \quad \Delta\rho/\rho \ll [\epsilon F_D, F_D^{-1}];$$

$$F_D \gg 1; \quad \epsilon/\beta_0 \ll [\epsilon F_D, F_D^{-1}].$$

A possible choice that would satisfy these conditions is $L_D = 50$ km and $L = 500$ km with velocities of the order of 0.5 cm s^{-1}, hence:

$$\beta_0 \sim 10^{-2}; \quad \epsilon F_D \sim 10^{-2}; \quad \Delta\rho/\rho \sim 10^{-3};$$

$$F_D^{-1} \sim 10^{-2} \ (F_D \sim 100); \quad \epsilon/\beta_0 \sim 10^{-3}; \quad \epsilon \sim 10^{-4}.$$

When the equations' validity conditions are all satisfied, the communicating regime still needs to be located in the basin. Knowing that $U = F_D w_0/(\beta_0^2 fH) \sim 0.025$ with $w_0 \sim 10^{-4}$ cm s^{-1} and $H \sim 4000$ m, the communication window will be situated out of the basin. As a matter of fact, this window is situated at the longitude where $\eta_2 \sim 0$, which, by means of (3.19), gives as localization $x = -1/U \sim -40$ or dimensionally $x_* = Lx \sim 20\,000$ km.

For this processes study, we shall violate the most restrictive constraint (3.11), which neglected the relative vorticity advection, and we shall take for spatial scales:

$$L = 200 \text{ km}, \ L_D = 20 \text{ km}, \tag{3.21}$$

with $H = 4000$ m, $H_1 = 400$ m and $H_2 = 3600$ m, hence:

$$\beta_0 \sim 0.04; \ \epsilon F_D \sim 0.1; \ F_D^{-1} \sim 0.01 \ (F_D \sim 100);$$

$$\Delta\rho/\rho \sim 10^{-3}; \quad \epsilon \sim 10^{-3}; \quad \epsilon/\beta_0 \sim 0.02.$$

Since $U \sim 0.15$ with these values, the window will be situated at a longitude of $x_* = 1300$ km, a value which, this time, is indeed included in the basin.

The window width, which is also a significant characteristic of the problem for a given perturbation $\Delta\eta_2$, will be given by (3.19):

$$\Delta x = \epsilon F_D/U\Delta\eta_2 \sim 1300 \text{ km} \quad (\Delta\eta_2 \sim 10).$$

The time scale is given by (3.7), i.e., $T = F_D/(\beta_0 f)$, of the order of $T \sim 0.8$ year ($f \sim 10^{-4}$ s^{-1}), with the aforementioned choice.

2) NUMERICAL MODEL AND TESTS

The equation to be solved numerically is Eq. (3.17) for the interface. Once the communicating stationary regime is achieved, the surface will be given by (3.20). The transient regime (3.18) for the free surface will not be solved.

The numerical scheme used is derived from a three time-level finite differences scheme developed by Eilbeck and McGuire (1975). Because of these three levels, it is necessary to apply a two-level scheme to the first time step, which is chosen as in Peregrine (1966).

Two simple applications will be proposed in preview. They will be useful on the one hand for testing the model and on the other for illustrating what will happen in the more complex case when the zonal flow $-Ux$ is different from zero and is a function of longitude.

(i) Solitary wave ($U = 0$). A solitary wave is a solution of equation (3.17) with $U = 0$. The transformation

$$\theta = x - Ct, \quad t' = t, \quad \partial(\ )/\partial t' = 0, \tag{3.22}$$

with η_2, $\eta_{2\theta}$ and $\eta_{2\theta\theta}$ tending to zero at infinity, leads to the solution

$$\eta_2 = \eta_{2\max} \operatorname{sech}^2\left[\left[\frac{-E_1\eta_{2\max}}{12E_2C}\right]^{1/2}(x - Ct)\right], \tag{3.23a}$$

with

$$C = -1 - (E_1/3)\eta_{2\max}, \tag{3.23b}$$

which keeps its form while propagating with velocity C.

This solitary wave solution exists only if the term under the square root is positive, i.e., when the non-

linear effect can be balanced by the dispersion. For the case $E_1 < 0$ ($H_1 < H_2$), E_2 always being positive, η_2 must satisfy $\eta_{2\max} < 0$ ($C < -1$) or $\eta_{2\max} > -3/E_1$ ($C > 0$); this last condition must be rejected, since the amplitude necessary for eastward propagation is too large.

Notice that eastward propagation is only possible if the perturbation exceeds a certain minimum value $|-3/E_1|$. This eastward propagation is possible in the BBM equation but not in the KDV one, because of the time derivative in the dispersive term.

If, on the contrary, this wave were propagating (eastward) in a positive constant zonal flow U, solution (3.23) would still be valid, but the velocity C would be given by

$$C = -1 + U - E_1/3\eta_{2\max}, \tag{3.24a}$$

and eastward propagation with small and positive perturbations would be possible, since the nonexistence interval of this solitary solution is shifted to another range of possible η_2 values, the zonal flow entailing an

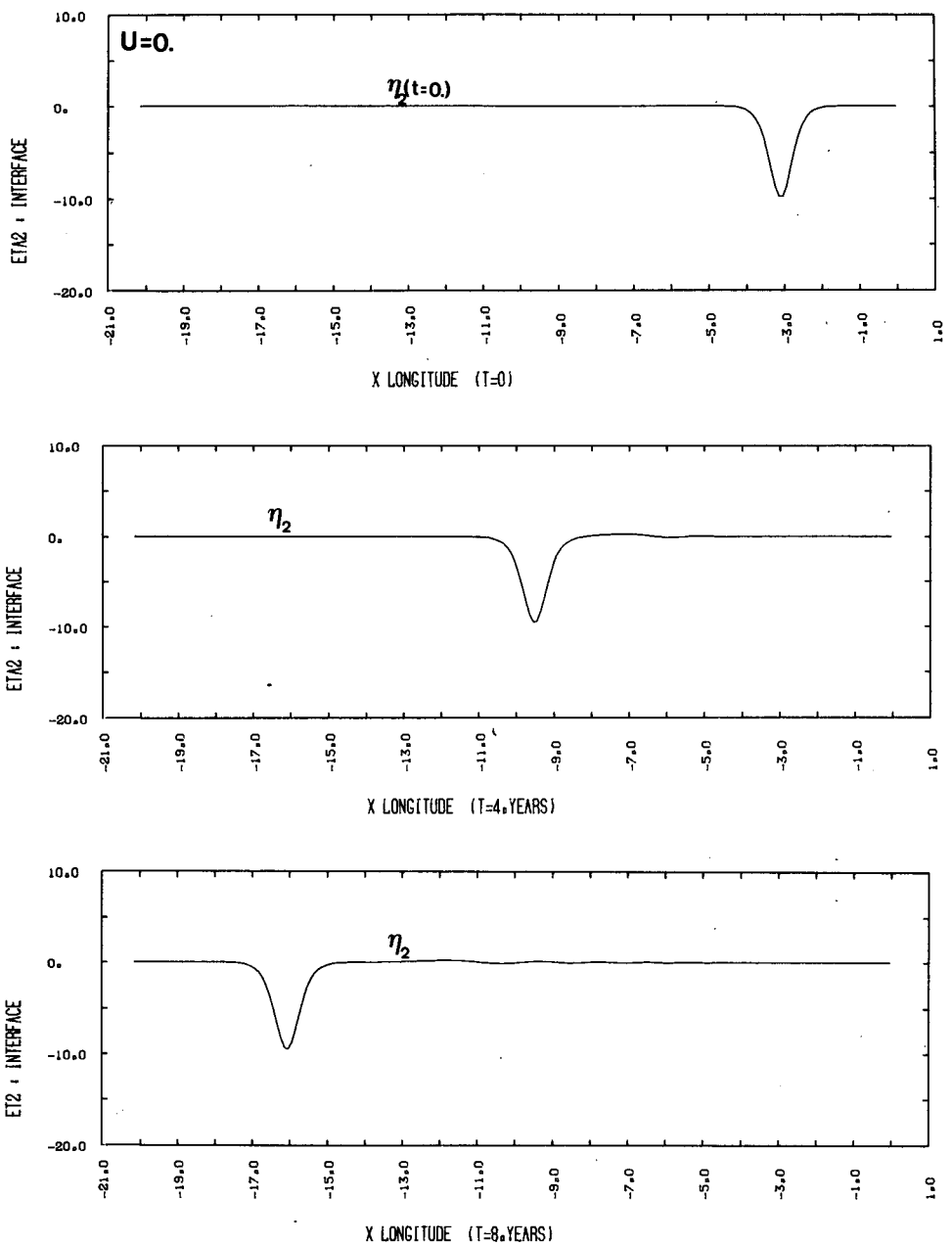

FIG. 6. Solitary wave propagation in the case when $U = 0$ [$\eta_{2\max} = -10$]. The curves represent the interface at different times.

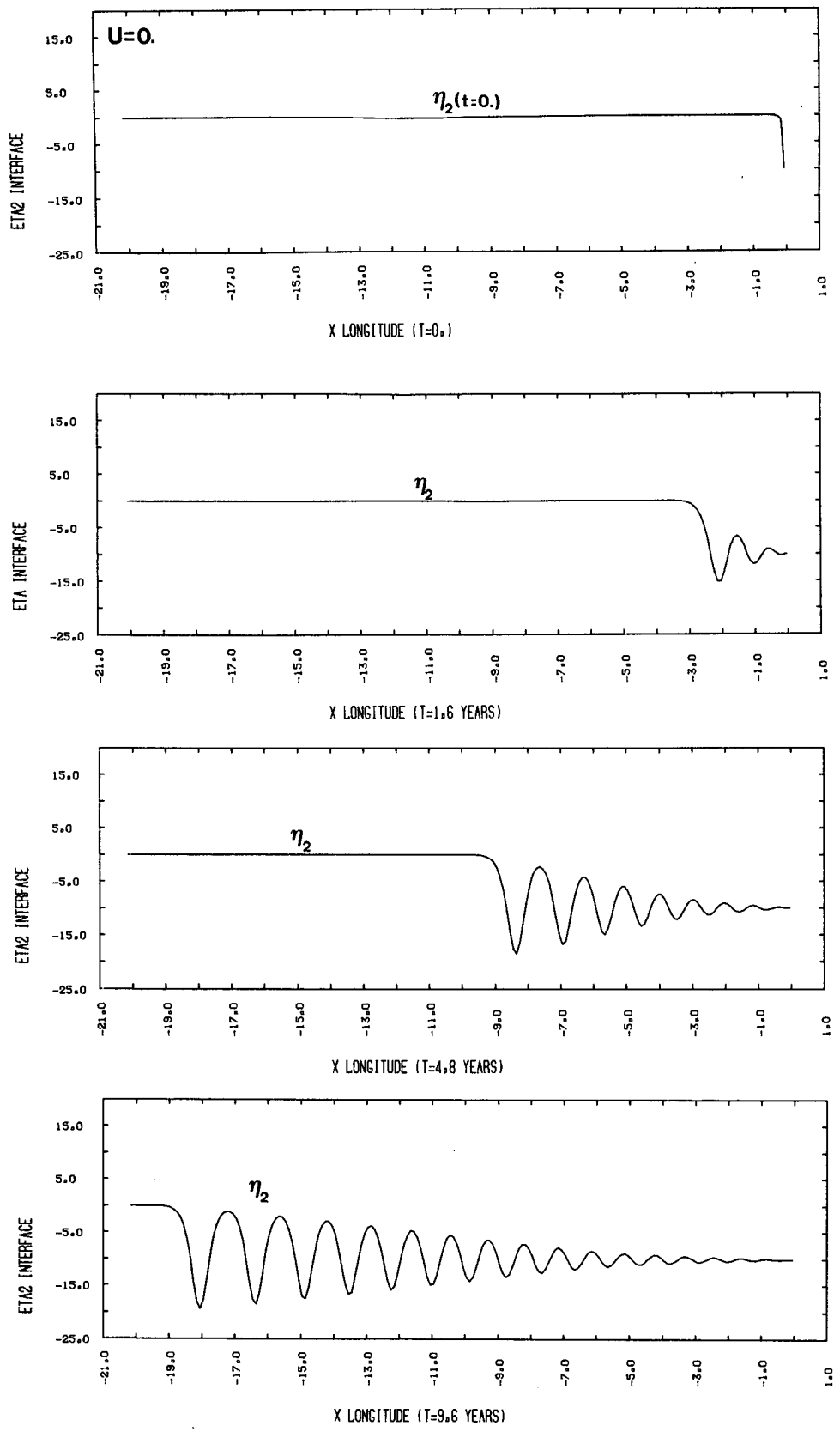

FIG. 7. Propagation of a front fixed at the eastern boundary with an amplitude of $\eta_2 = -10$, which breaks into solitary waves with time.

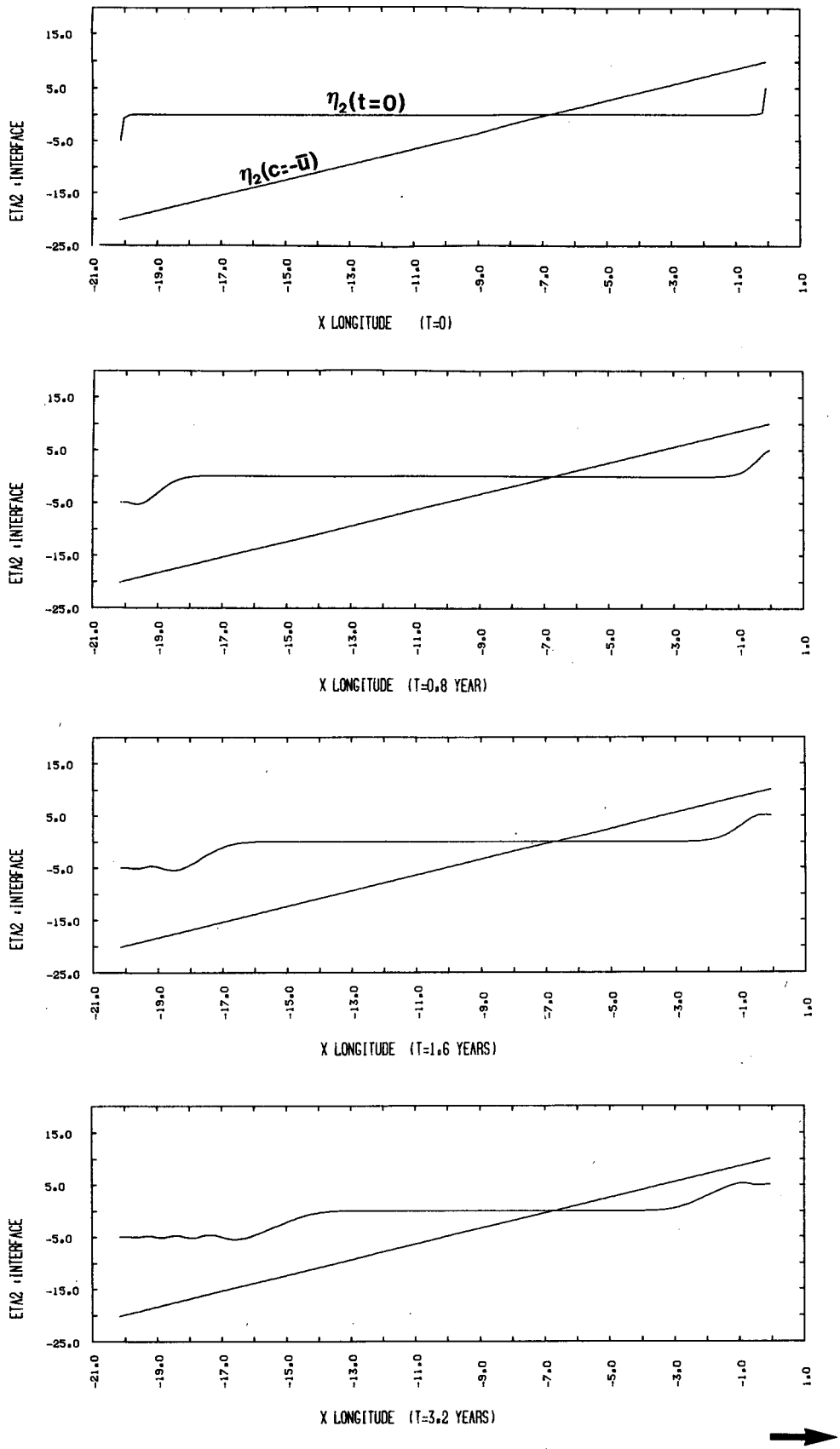

FIG. 8. Time evolution of the interface displacement along the zero wind stress curl line under the influence of perturbations generated on both boundaries. The tilted straight line is the steady communicating solution. At $t = 0$, the interface is horizontal and evolves toward the steady communicating solution.

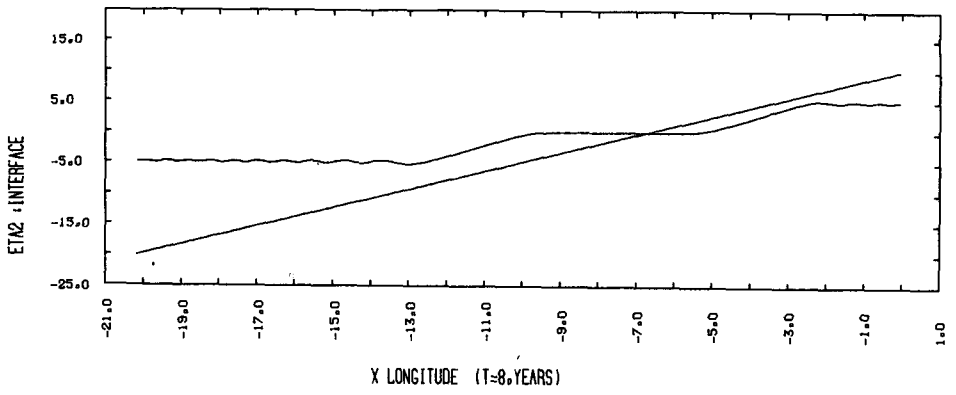

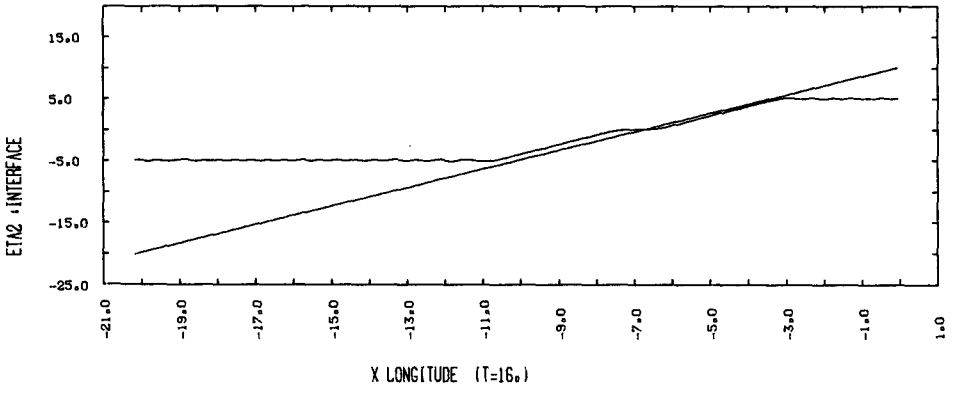

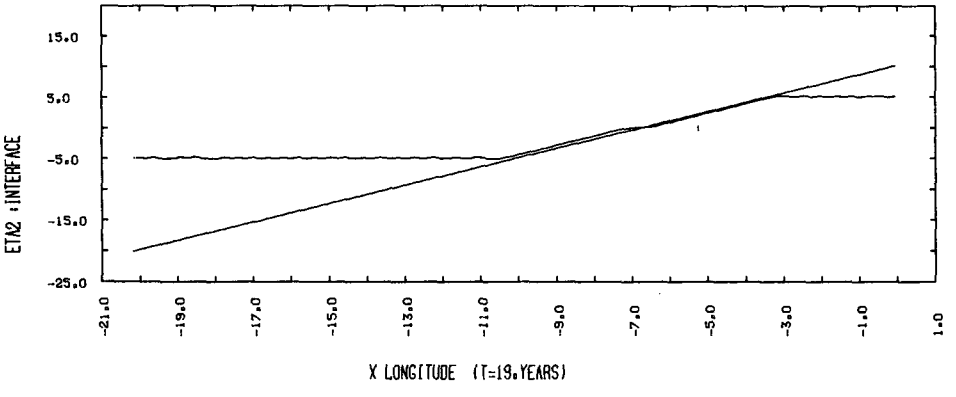

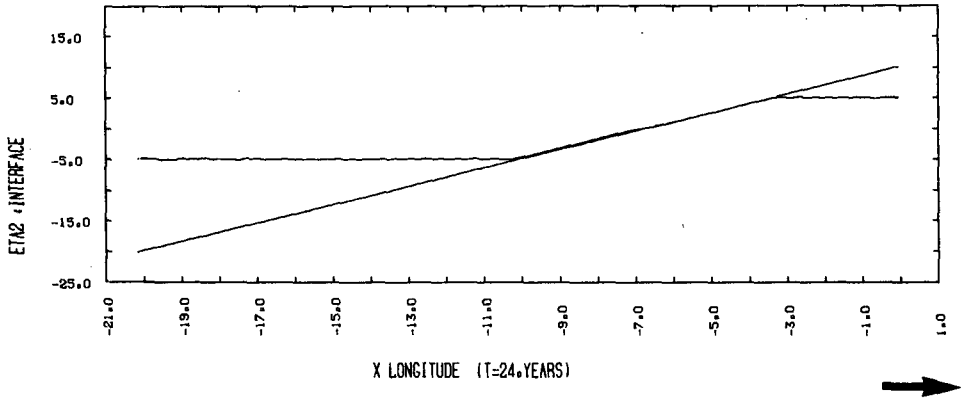

FIG. 8. (*Continued*)

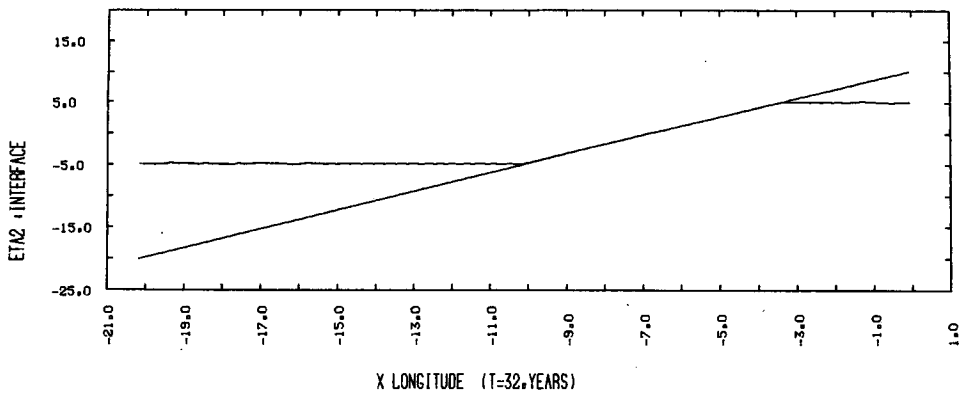

FIG. 8. (*Continued*)

eastward transport of these waves. This interval for the case $E_1 < 0$ is given by

$$\eta_{2\max} > 3(1 - U)/(-E_1) \quad \text{and} \quad \eta_{2\max} > 0, \quad (3.24b)$$

or

$$\eta_{2\max} < 3(1 - U)/(-E_1) \quad \text{and} \quad \eta_{2\max} < 0. \quad (3.24c)$$

Now we test this solitary wave in the numerical model by disturbing the interface at the initial instant by a deformation given in (3.23). A maximum amplitude $\eta_{2\max} = -10$ has been taken with the choice of preceding parameters. Figure 6, where η_2 is represented as a function of longitude, illustrates this wave propagation through a basin of width 4000 km. The eastward propagation, shown at two equal time intervals on this figure, keeps the wave form at constant speed, as expected by theory, and provides validation for the numerical model used.

(ii) Heaviside perturbation ($U = 0$). We test a second case in which an interface level difference is imposed initially at the eastern boundary and remains imposed constant in time on this boundary. In this type of equation, any perturbation satisfying (3.24) inevitably breaks into solitary waves; therefore, the initial condition is chosen negative for these waves to appear. Figure 7 represents the time evolution of this front imposed on the eastern boundary. The appearance of a solitary wave-train can effectively be observed, with decreasing amplitudes propagating westward. During propagation, these waves will break away from the front and become isolated entities, each propagating at its own velocity given by dispersion relation (3.23b), the largest ones at the edge of the front propagating faster.

3) COMMUNICATING SOLUTION WITH DEEP NORTHWARD FLOW

The parametric choice in the preceding section, imposed by the presence of a communicating window in the basin, will be applied with the variable mean zonal flow function of x. To perform the stationary state adjustment, however, perturbations on the initial state, in which the interface is horizontal, must first be specified. In doing so, the northward flow solution obtained in SA, in which the interface thickness between moving layers is deeper on the western boundary than on the eastern boundary, will be considered. Thus, in this application, the interface perturbation will be taken as constant and negative on the western boundary (which is equivalent to a warming) and as positive on the eastern boundary [equivalent to a cooling, which corresponds to the analysis carried out by Luyten et al. (1985) in this region]. Equation (3.17) is solved numerically this time with the mean current $-Ux$ a function of longitude. Figure 8 represents the interface time evolution. The sloping line is the stationary solution given by relation (3.19). It can be observed that both eastern and western fronts propagate toward the communicating window, although the eastern front is dominated by Rossby wave speed, whereas the western one is dominated by the mean zonal flow. During propagation, these fronts become less steep, the speed of perturbations is larger for lower amplitudes (due to nonlinear wave propagation), and, reducing speed slowly, they adjust to the stationary solution in which the baroclinic wave speed balances the mean zonal current. This balance is reached after about 20 years, i.e., the time scale characteristic of wind-forced large-scale circulation. The communicating window width is given by the difference of depths fixed on both boundaries, given in paragraph (i) by $\Delta x = 1300$ km. The surface is determined from (3.20), and the final steady equilibrium solution is represented by Fig. 9. A southward flow in the surface layer and a northward flow in the deeper layer are indeed observed. The communicating solution of the ventilated thermocline equations in SA has thus been reached by a rather realistic transient regime.

4) COMMUNICATING SOLUTION WITH DEEP SOUTHWARD FLOW

The solution of a southward flow in the deeper layer (Pedlosky 1984) does not appear in this analysis at first glance; however, it is included. As a matter of fact, changing the sign of E_1, i.e., choosing $H_1 > H_2$, enables

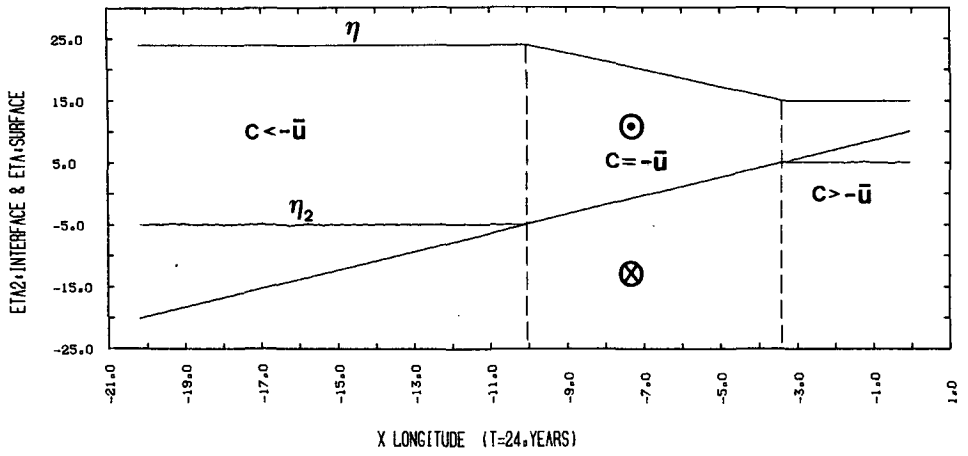

FIG. 9. Final steady solution obtained from the transient regime representing the interface and free surface displacements. Northward current in the deeper layer and southward flow in the upper layer.

us to change the sign of the stationary solution slope. A similar transient regime, but with opposed perturbations on both boundaries, would make it possible to reach this solution. But in order to make both northward and southward solutions appear simultaneously, it is sufficient to keep the term in $\eta_2{}^2$ in the baroclinic Rossby wave nonlinear phase speed (see paragraph 3a). Figure 10 shows the effect of this additional term on the northward communicating stationary solution (very small effect justifying the approximation used). It makes this second mode appear with deep southward flow in layer 2, which is inaccessible for the values of depths chosen. However, although this term is very small, it can become significant when both layer thicknesses are close. Let us suppose that they are equal ($H_1 = H_2$, possible in LPS models), the term in η_2 becomes zero ($E_1 = 0$), and the term in $\eta_2{}^2$ balances the mean zonal current variation. The parabola of Fig. 11 then represents both modes of the communicating stationary state. A maximum can be observed west, which represents the boundary found in SA and Pedlosky (1984) and corresponds to the Rossby wave speed maximum (the term in η_2 being the first term of this wave speed limited development).

Notice that this maximum also exists for different thickness values: pushed westward out of the domain, it does not appear in Fig. 10. A transient regime for a southward flow has been done in this case and is illustrated in Fig. 11. The perturbation is applied only on the eastern boundary and represents a warming. A cooling at this boundary would lead to a northward flow in this particular case, where $H_1 = H_2$.

5) SOLITARY WAVES

In these solutions, the solitary waves of the preceding equation study did not appear. The dispersive term only played the role of stabilizing initial fronts in these cases and enabled us to easily solve the equations numerically. The occurrence of these waves depends principally on the initial deformation (sign and form). In fact, in applying different initial conditions on

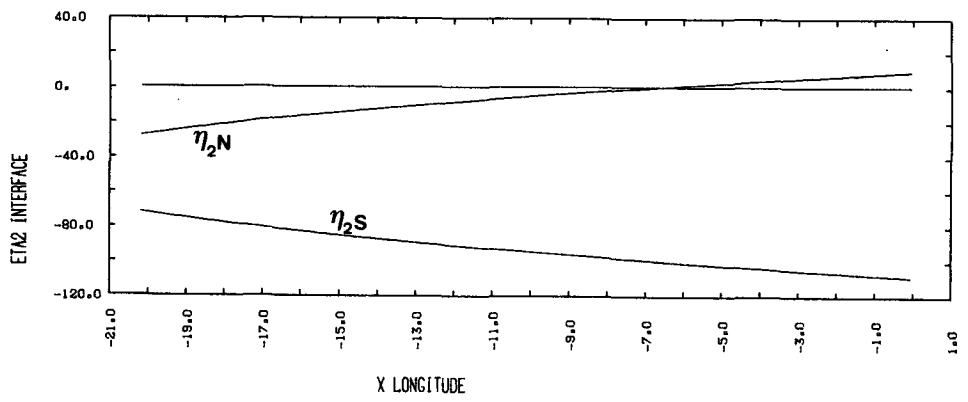

FIG. 10. Stationary communicating solution that represents the two internal modes by considering the quadratic term in the Rossby wave speed: η_{2N} northward solution and η_{2S} southward solution (Pedlosky 1984).

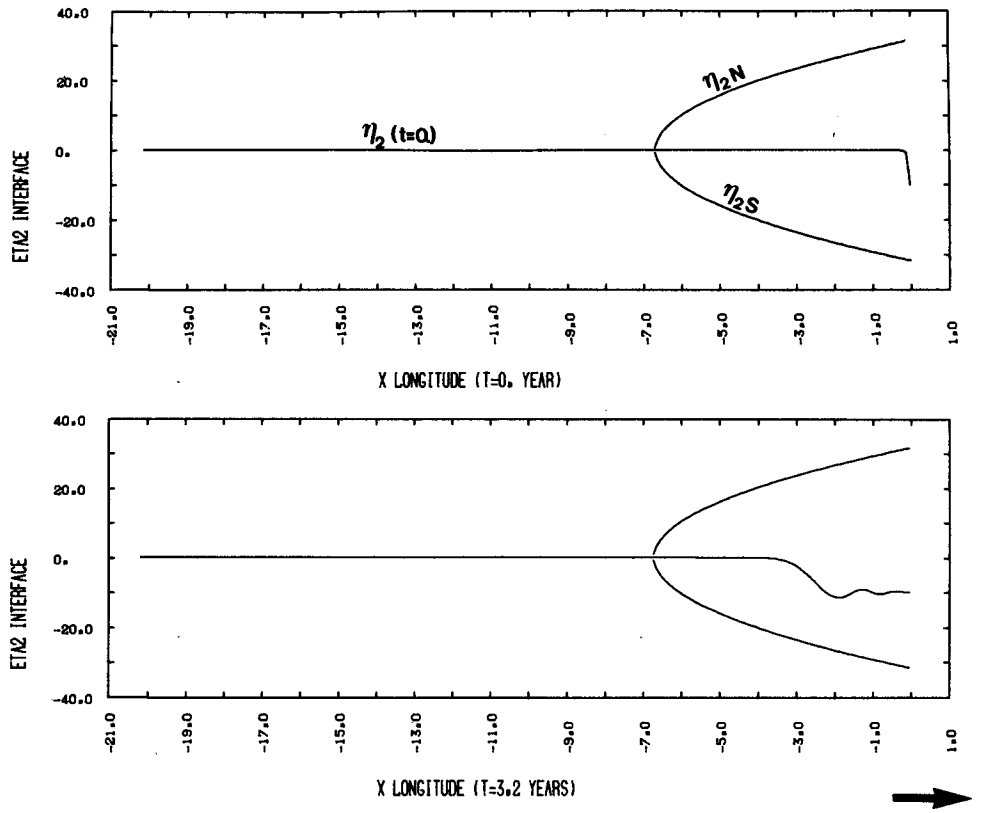

FIG. 11. Transient regime for a southward steady solution in the deeper layer that considers the quadratic term in the Rossby wave in the case when $H_1 = H_2$. The parabola represents the two steady solutions and shows the maximum of phase speed that limits the communicating window westward.

boundaries, the interface will react toward other states, more complex than that of the communicating solution. In imposing a positive disturbance on the western boundary, for example, this front will propagate eastward, decomposing into solitary waves transported eastward by the zonal flow $-Ux$. Figure 12 illustrates this outbreak of solitary waves; but as a result of the variation of the zonal current $-Ux$, these waves are slowed down when they get closer to the communicating window and are arrested there when the zonal flow has decreased to the point of opposing to the velocity of these waves. Inequality (3.24b) can no longer be verified, i.e., dispersion can no longer balance nonlinear propagation. Notice that long waves propagate toward the window while short waves propagate away from it; however, since the group velocity of all waves is zero where $u = -c$, energy is accumulated at these points. Notice that from (3.24b), by increasing the amplitude of the perturbation, solitary waves would be able to cross this region. However, to avoid these pathological cases, other processes must be taken into account to solve the problem, such as, for example, dissipation of energy or advection of relative vorticity.

4. Discussion

The interpretation of the cross-gyre internal modes found in Pedlosky (1984) and Schopp and Arhan (1986) in terms of an arrested nondispersive baroclinic Rossby wave by a barotropic mean zonal current along the zero wind-stress curl line shows the importance of the gyres' common boundary, which happens to be the place where information can be generated and spread toward the interior of each gyre and which justifies the specification of the outcropping line in the subpolar gyre in SA. The time-dependent study presented suggests a process able to generate currents connecting the gyres from an ocean at rest or from an ocean with no initial mass transfer. It therefore validates the particular stationary internal mode solution of the ventilated thermocline, and the northward flow solution proposed in SA as a transfer mechanism of Mediterranean water toward high latitudes.

The effect of the nonlinear potential vorticity advection term has been neglected in this process study. Were this term linearized around a mean current, other communication possibilities would appear, such as stationary solitary waves in a zonal current, communication then having the form of cells along the zero wind curl line. Moreover, it would enable a connection between the eastern and western regimes and would prevent energy from being blocked in the communicating window.

For reasons of simplicity, the dispersion meridional component has been neglected. This is an unrealistic

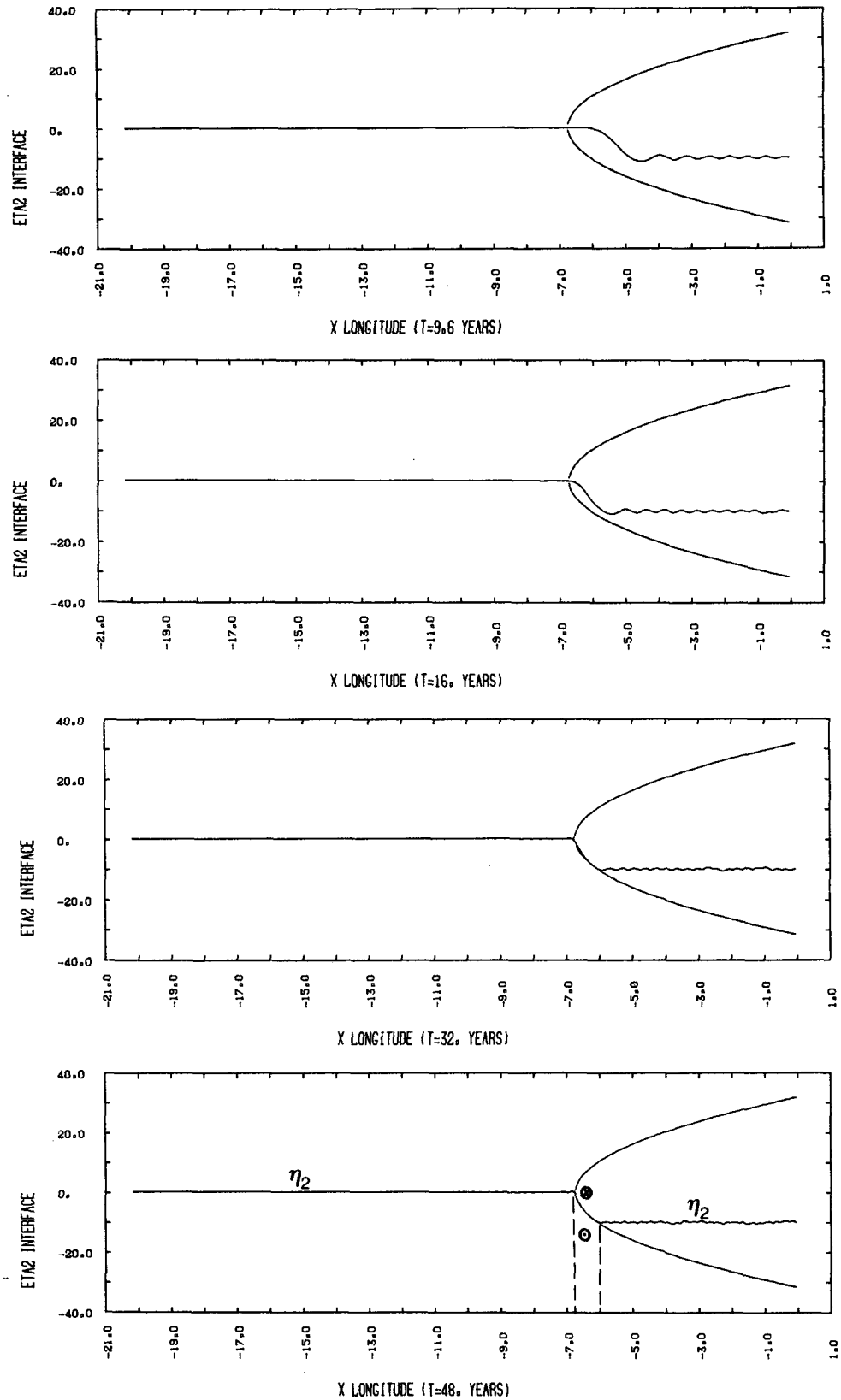

FIG. 11. (*Continued*)

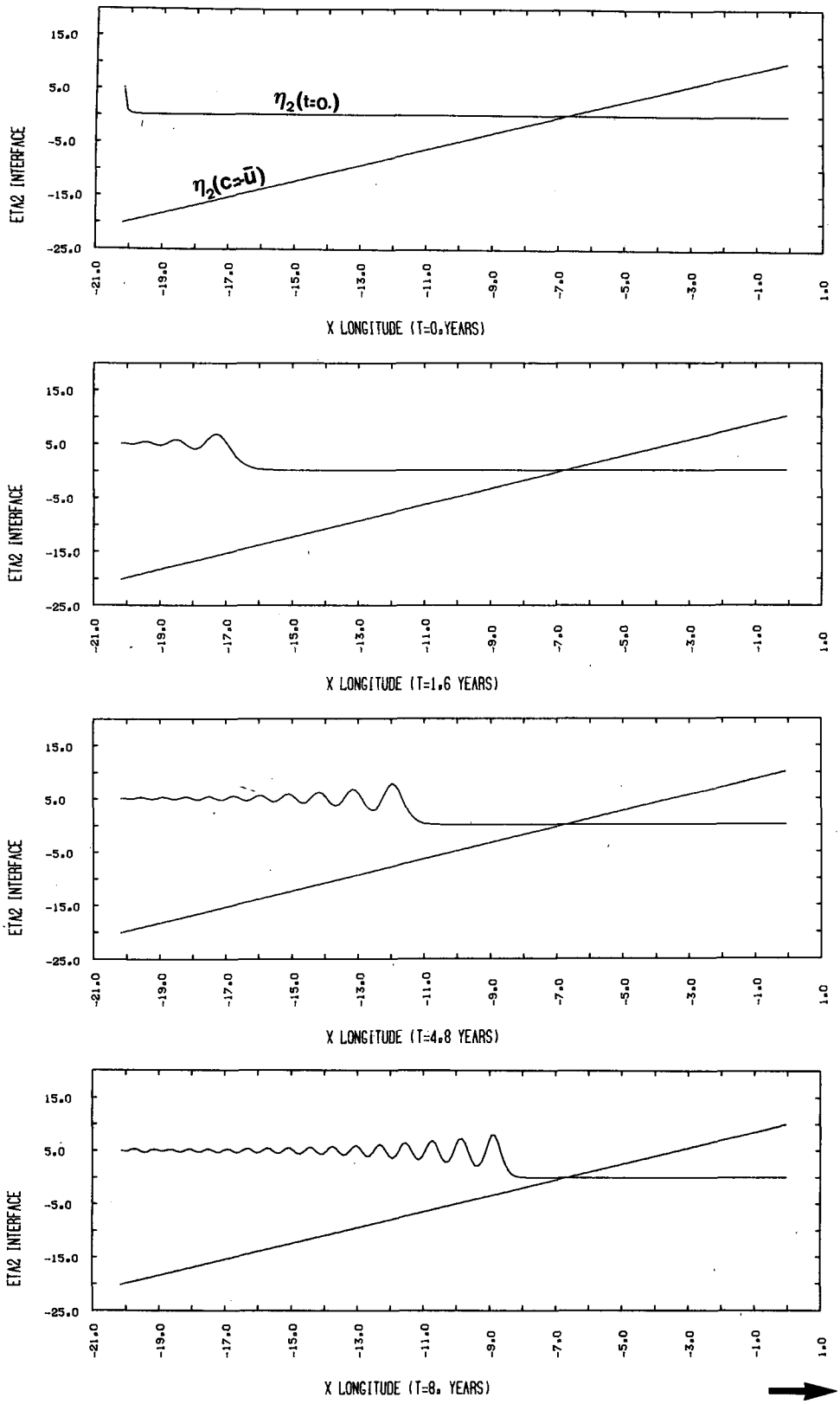

FIG. 12. Case with a positive perturbation at the western boundary. Appearance of solitary waves blocked in the vicinity of the communicating window ($u = -c$).

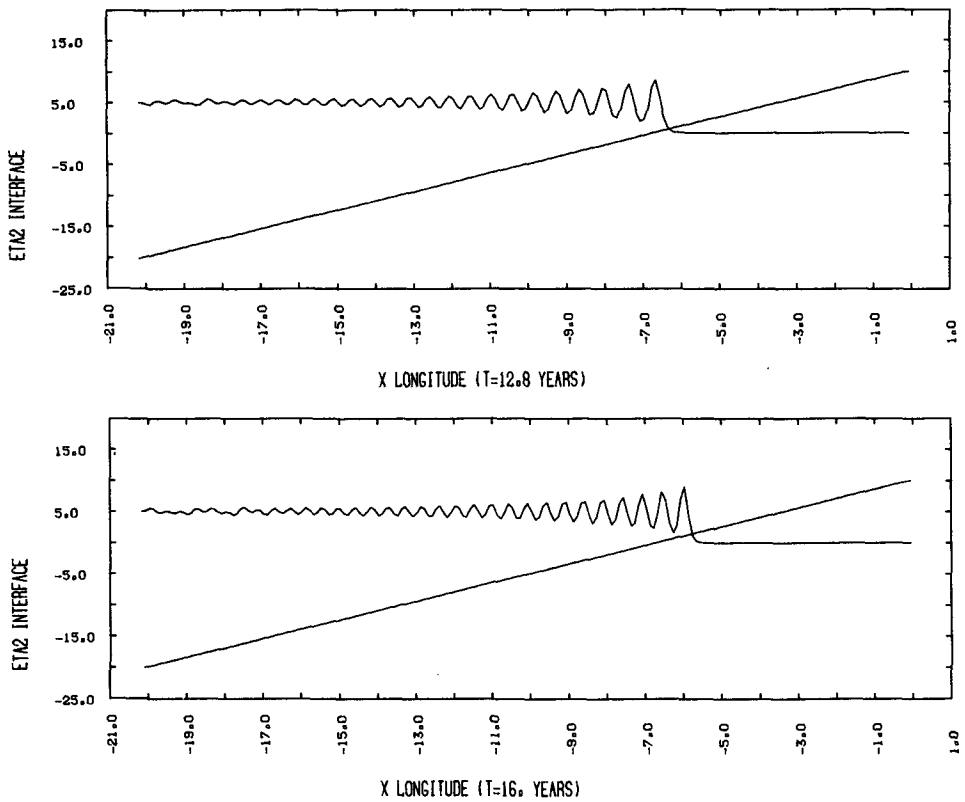

FIG. 12. (*Continued*)

approximation of the model, since this component is partly responsible for evacuation of energy stored at the control point. Likewise, forcing the model by thermohaline processes (of upwelling type) at the interface would probably be more physical than imposing interface displacements. Finally, since the equations are valid for the whole basin, it should be possible to use them to study realistic transient regimes.

Acknowledgments. I would like to thank Dr. J. Pedlosky, who brought into being and supported this work during my stay at WHOI, Woods Hole. This work was also supported by a DGRST scholarship. Many thanks to Lee Panetta and David Straub for improving the English.

REFERENCES

Benjamin, T. B., J. L. Bona and J. J. Mahony, 1972: Model equations for long waves in nonlinear dispersive systems. *Phil. Trans. Roy. Soc. London,* **272A,** 47–78.

Charney, J. G., and G. R. Flierl, 1981: Oceanic analogues of large-scale atmospheric motions. *Evolution of Physical Oceanography.* B. A. Warren and C. Wunsch, Eds., MIT Press, Chap. 18, 504–548.

Dodd, R. K., J. C. Eilbeck, J. D. Gibbon and H. C. Morris, 1982: *Solitons and nonlinear wave equation.* Academic Press, 630 pp.

Eilbeck, J. C., and G. R. McGuire, 1975: Numerical study of the regularized long wave equation 1: Numerical methods. *J. Comput. Phys.,* **19,** 43–57.

Korteweg, D. J., and G. de Vries, 1895: On the change of form of long waves advancing in a rectangular channel, and on a new type of long stationary waves. *Phil. Mag.,* **39**(5), 422–443.

Luyten, J. R., and H. Stommel, 1985: A beta-control of buoyancy driven geostrophic flows. *Tellus,* **38A,** 88–91.

——, and ——, 1986a: Gyres driven by combined wind and buoyancy flux. *J. Phys. Oceanogr.,* **16,** 1551–1560.

——, and ——, 1986b: Experiments with cross-gyre flow patterns on a beta-plane. *Deep-Sea Res.,* **33A,** 963–972.

——, and ——, 1986c: Some examples of finite amplitude forced flow patterns on a beta-plane. (manuscript).

——, J. Pedlosky and H. Stommel, 1983: The ventilated thermocline. *J. Phys. Oceanogr.,* **13,** 292–309.

——, H. Stommel and C. Wunsch, 1985: A diagnostic study of the Northern Atlantic subpolar gyre. *J. Phys. Oceanogr.,* **15,** 1344–1348.

Pedlosky, J., 1984: Cross-gyre ventilation of the subtropical gyre: An internal mode in the ventilated thermocline. *J. Phys. Oceanogr.,* **14,** 1172–1178.

——, 1987: *Geophysical Fluid Dynamics.* Springer-Verlag, 710 pp.

Peregrine, D. H., 1966: Calculation of the developpement of an undular bore. *J. Fluid Mech.,* **25,** 321–330.

Rhines, P. B., 1986: Vorticity dynamics of the oceanic general circulation. *Ann. Rev. Fluid Mech.,* **18,** 433–497.

Schopp, R., and M. Arhan, 1986: A ventilated middepth circulation model for the Eastern North Atlantic. *J. Phys. Oceanogr.,* **16,** 344–357.

Whitham, G. B., 1974: *Linear and Nonlinear Waves.* Wiley & Sons, 636 pp.

Williams, G. P., and T. Yamagata, 1984: Geostrophic regimes, intermediate solitary vortices and jovian eddies. *J. Atmos. Sci.,* **41,** 453–478.